Sensor and Simulation Notes

Note 478

July 2003

Experimental Studies of Scale-Model and Full-Scale IRAs Mounted on Parachutes

Lanney M. Atchley and Everett G. Farr
Farr Research, Inc.

Larry L. Altgilbers
U. S. Army / Space and Missile Defense Command

Abstract

We investigate here a number of variations of the Para-IRA, which is an Impulse Radiating Antenna configured for parachute delivery. We consider first two scale models of the Para-IRA with aluminum reflectors, and then we consider a full-scale version built from fabric. In the scale models, we first investigate the effect of using a large *F*/*D* ratio in an IRA. We then investigate the effect of using a trimmed reflector, with portions of the reflector removed that contribute destructively to the radiated field. Two scale model antennas with aluminum reflectors were built with *F*/*D* = 1.0 and with radius = 46 cm (18 in.). These antennas were configured with so-called "non-floppy" feed arms, which are contained entirely within the aperture. One antenna had a complete circular reflector, and the other had a trimmed reflector. Experimental data from these two designs are compared to data from earlier designs. We also built and tested a fabric version of the Para-IRA, which had a number of improvements over earlier versions.

I. Introduction

During the course of the development of the parachute mounted Impulse Radiating antenna, or Para-IRA, we found the need to introduce a number of variations on the standard IRA design [1]. In this note, we quantify the effect of these variations by building and testing two scale models of the Para-IRA, comparing the results to earlier designs. In particular, we study the effect of a large F/D ratio in an IRA, and we also study the effect of trimming the aperture. In addition, we built and tested a full-size fabric version of the Para-IRA that is more refined than that developed in [1].

First, we investigate the effect of using a large F/D ratio, which is helpful in mechanically stabilizing the Para-IRA. A larger F/D ratio allows the weight of the Marx generator to be positioned lower and farther away from the reflector, giving the entire structure a lower center of gravity. The lower center of gravity and longer pendulum arm reduces parachute oscillation resulting in a more predictable target area. To study this effect, we built the IRA-5, which has $F/D = 1$. Data from this new antenna is directly comparable to the IRA-4 [3], which has $F/D = 0.5$, but is otherwise identical to the IRA-5.

Next, we investigate the effect of trimming the shape of the parabolic reflector, to eliminate the portion of the reflector that contributes destructively to the radiated field. Trimming the aperture becomes more important when the feed arms are positioned in the so-called "non-floppy position", with the outside edge of the feed arm aligned with outer edge of the reflector. Aperture trimming was studied theoretically in [2], and we provide here experimental data for comparison. In [2], it was found that moving the feed arms to the non-floppy position reduces aperture height, however, trimming the aperture allows one to recover the lost field. In support of this effort, we built the IRA-5b, which is identical to the IRA-5, except that the aperture is trimmed. Note that a trimmed aperture can be incorporated easily into a fabric reflector by substituting some non-conducting fabric for the conducting fabric in the region of interest.

We also take a second look at old data relating to the effect of feed arm position. In the standard feed arm position, such as that used in the IRA-3, the electrical center of the feed arm is aligned with the edge of the reflector. If the standard configuration were used in a Para-IRA, the feed arms would be literally floppy, because the outside edge of the feed arm could not remain under tension. A better approach is to place the feed arms so their outside edge intersects the outer edge of the reflector. This configuration, called the "non-floppy" configuration, has been studied theoretically in [2], and experimentally in [3]. We present here a careful comparison of the effect of switching from standard feed arms to non-floppy. To do so, we compare the IRA-3, with standard feed arms, to the IRA-4, with non-floppy feed arms.

Finally, we built and tested a full-scale version of the Para-IRA that was 1.22 meters (4 feet) in diameter, and tested it while mounted on a wooden frame. We present data on this version and compare to earlier versions.

We begin by describing the IRA-5 and IRA-5b.

II. Description of the IRA-5 and IRA-5b

The IRA-5 antennas are 46-cm diameter scale models of the 1.22-meter diameter Para-IRA. We use solid metal reflectors because their shape and tolerance can be controlled more accurately than fabric. The IRA-5 has a focal length equal to its diameter, and the reflector is machined aluminum. The four feed arms are copper plate; each positioned ±30˚ from vertical. These feed arms are positioned in the non-floppy configuration, in which the outside edge of the feed arm is aligned with the rim of the reflector. The ground plane is positioned in a plane of symmetry, and it is fabricated from aluminum plate. The fabric Para-IRA does not use a ground plane, but the ground plane adds structural support to the metal scale model without affecting performance.

We terminated the feed arms at the reflector in three impedances – open, short, and 200 ohms – during the antenna evaluation. The input to the antenna is a 50-ohm female SMA connector feeding a splitter balun, which is located behind the reflector. The output of the splitter is two 100-ohm, 0.141-inch-diameter semi-rigid cables that drive the two pairs of feed arms. We show development drawings of the two IRA-5 models in Figure 2.1.

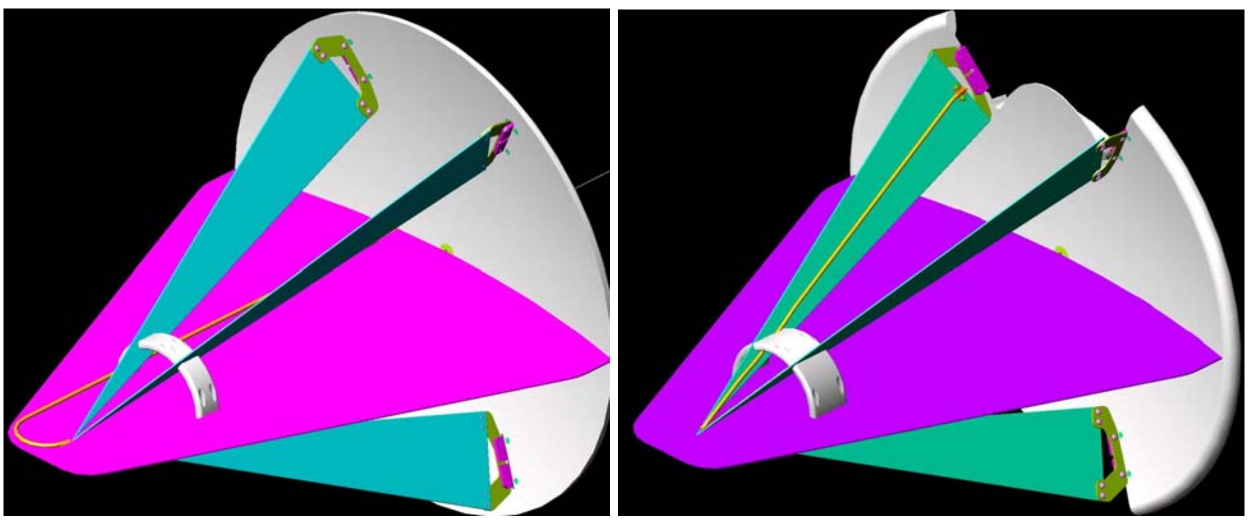

Figure 2.1. Drawing of IRA-5 (left) and IRA-5b (right).

The IRA-5b differs from the IRA-5 solely in the reflector shape. In Figure 2.1 one sees a small portion removed from the top of the IRA-5b. There is a mirror-image portion, not seen in the figure, removed from the bottom.

The developmental drawings in Figure 2.1 vary slightly from the final versions. Both antennas use the wider support ring near the apex shown on the IRA-5b. In addition, both antennas have the smoothly rounded reflector rim shown on the IRA-5b. We show the prototypes mounted for testing on tripods in Figure 2.2.

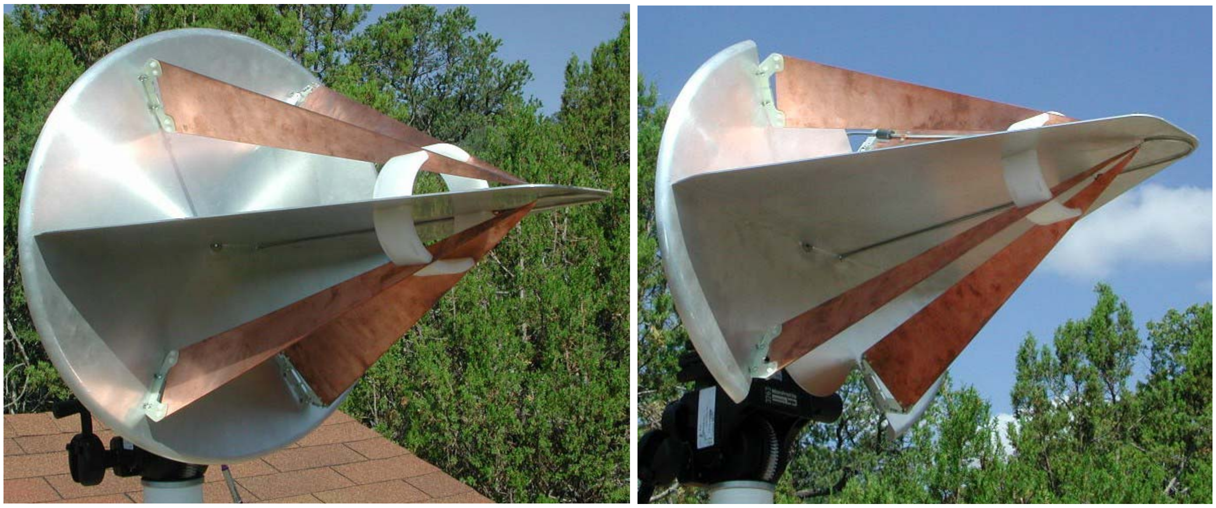

Figure 2.2. IRA-5 (left) and IRA-5b (right) set up for testing.

In Figure 2.3 we show the IRA-3 and IRA-4 for comparison. The IRA-3 differs from the IRA-4 and IRA-5 in the alignment of the feed arms. In the IRA-3, the *electrical centers* of the feed arms are aligned with the outside edge of the reflector (standard or floppy feed arms). On the other hand, in the IRA-4 and IRA-5 the *outside edges* of the feed arms are aligned with the outside edge of the reflector (non-floppy feed arms). IRAs with flexible feed arms, such as the Para-IRA, normally require non-floppy feed arms.

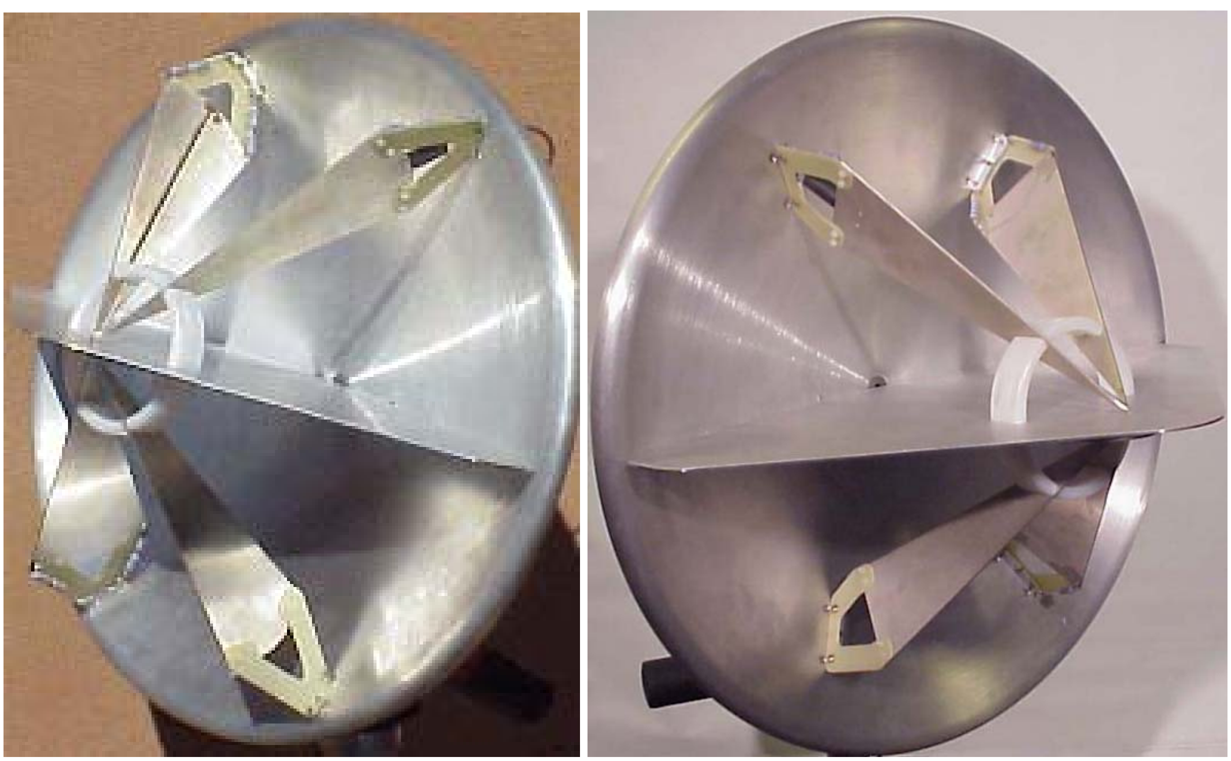

Figure 2.3. The IRA-3 (left) and IRA-4 (right).

III. Design Details of the IRA-5 and IRA-5b

The IRA-5 is designed to test the effect of using a large F/D ratio. The requirement for the long F/D ratio comes from early aerodynamic studies of the stability of Para-IRA during descent. The early results suggested that using $F/D = 0.5$, as in an IRA-3 or IRA-4, results in a descent with less stability and more swinging. A longer focal length is more aerodynamically stable, because it positions the weight of the generator further from the parachute canopy.

As noted earlier, the Para-IRA (and thus the IRA-5) must have non-floppy feed arms to maintain the correct feed arm position. Another requirement for the feed arms of an IRA in general, is that the feed arm length should be a perfect triangle out to a distant of one focal length from the focus. The increased length of the feed arms increases the aperture blockage in the IRA-5, relative to earlier models.

We built the IRA-5b to test Dr. Scott Tyo's theory on removal of destructively contributing reflector material. The available theory shows that the far field in the two principal planes is determined by the y-component of the electric field everywhere in the aperture. For most of the aperture, the y-component of the electric field is all oriented in the same direction. However, for a portion of the aperture between the feed arms, the y-component of the electric field is oriented in the opposite direction. If one eliminates the areas of the aperture where E_y is oriented in the wrong direction, the prompt radiated response from the IRA is predicted to improve by 7.5%. To find these areas of destructive contribution, we calculate the electric field in the projected aperture. We do this by solving the Laplace equation for the TEM feed structure and then by taking the gradient of the resulting electric potential.

The portion of the aperture that contributes destructively to the radiated field is shown in Figure 3.1. The portion of the aperture above the heavy line makes a negative contribution to the radiated field. Thus, over that portion of the aperture, we replace the conducting reflector with a non-conducting fabric, in order to improve performance. In the IRA-5b, we simulate this by trimming the aperture shape. In Figure 3-2 we show the exact area removed from the IRA-5 reflector

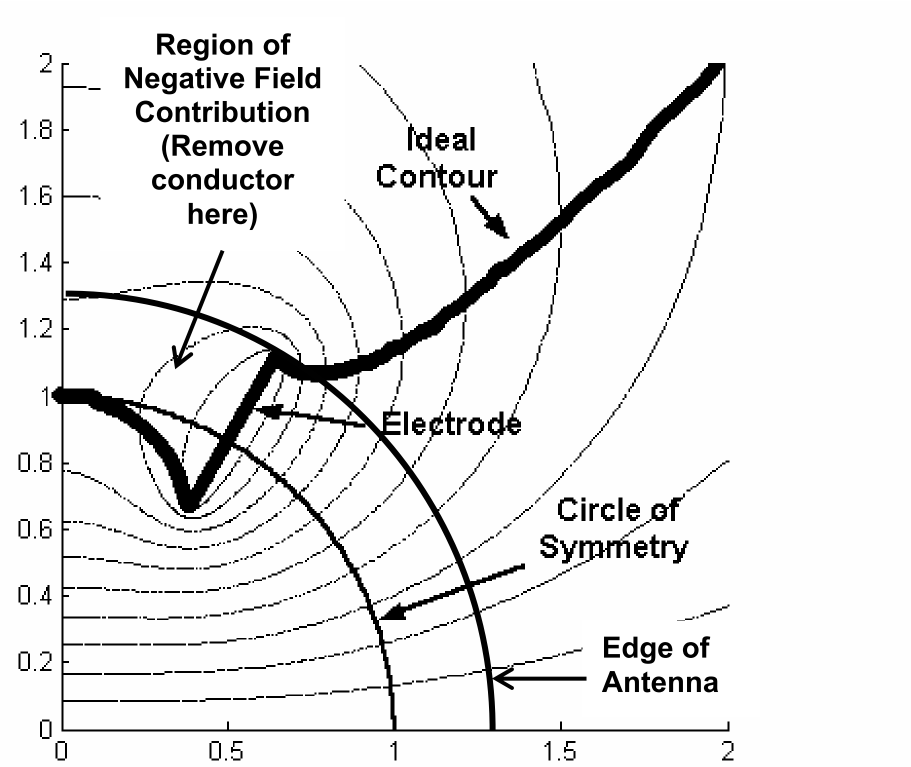

Figure 3.1. Sketch of the aperture fields of one-quarter of an IRA reflector. Note the Region of Negative Field Contribution, where conductor in the reflector should be removed.

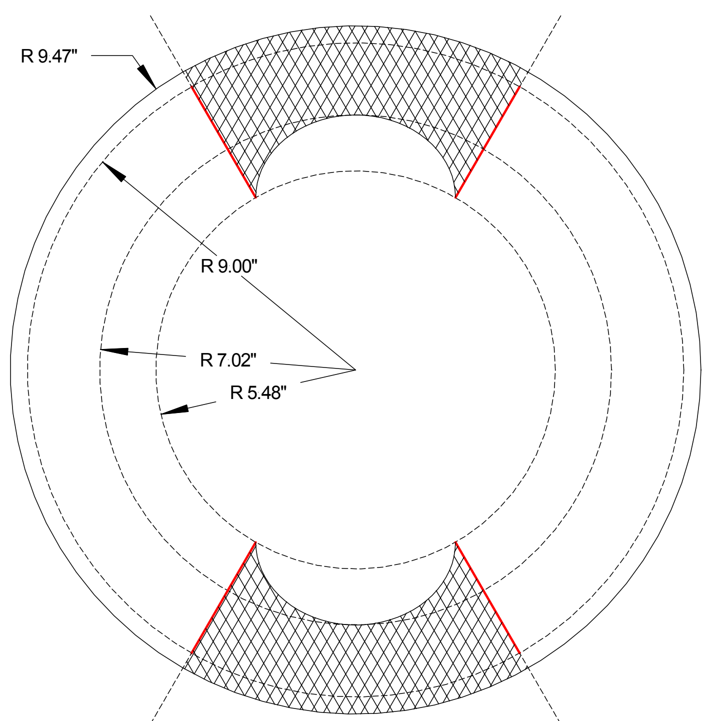

Figure 3-2. Shaped IRA-5 dish with removed area crosshatched.

IV. Antenna Measurements of the IRA-5 and IRA-5b

We began by measuring the impedance profile of the two IRA-5s using time domain reflectometry (TDR). The impedance of the IRAs is shown in Figure 4.1. These two profiles show that the impedance discontinuity at the splitter is negligible – only 2 ohms. The impedance discontinuity at the feed point is about 7 ohms for the IRA-5 and about 3 ohms for the IRA-5b. The better impedance match of the IRA-5b may slightly improve its gain at high frequencies. In either case, the impedance match is reasonable.

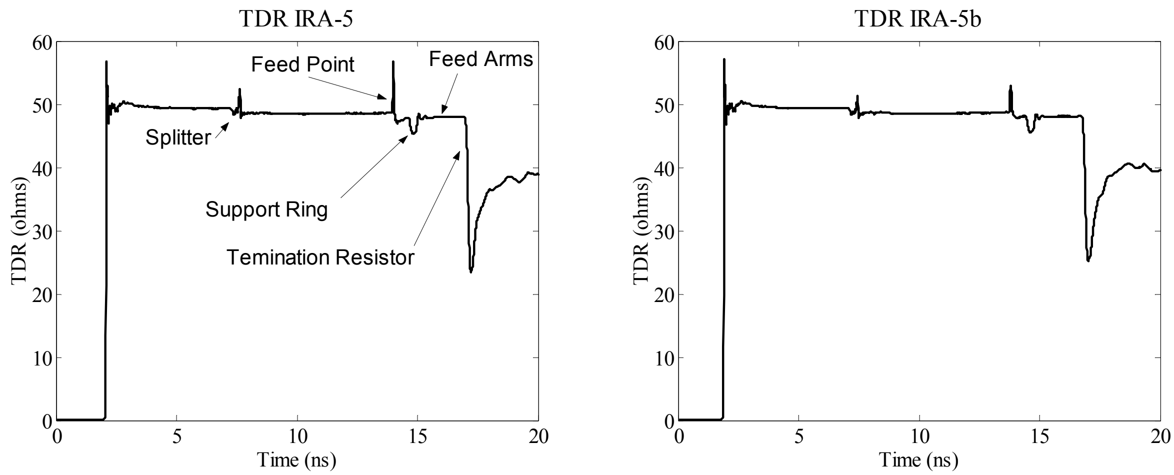

Figure 4.1. Impedance profile of the IRA-5 and IRA-5b.

Next, we tested the IRA-5 and the IRA-5b on our time domain antenna range, as shown in Figure 4.2. A Farr Research model TEM-1-100 sensor was driven by a Picosecond Pulse Laboratory (PSPL) Model 4015C pulse generator (4 volts peak, 20 ps risetime). The signal received by the IRA-5 is detected by a Tektronix TDS8000 digital sampling oscilloscope (DSO) with an 80E04 sampling head. The TEM-1-100 sensor and the IRA-5 are separated by approximately 10 meters and are about 3 meters above the ground.

By measuring the boresight gain of the IRA-3, IRA-4, and IRA-5, we can test the effect of the feed arm position (floppy vs. non-floppy) and F/D ratio (0.5 vs. 1.0). All three sets of data are plotted in Figure 4.3. We can see that there is a clear advantage in using a smaller F/D ratio and in using the standard feed arm configuration. Both of these have been compromised in order to build the Para-IRA, so we are now able to use this graph to quantify the effect of these compromises.

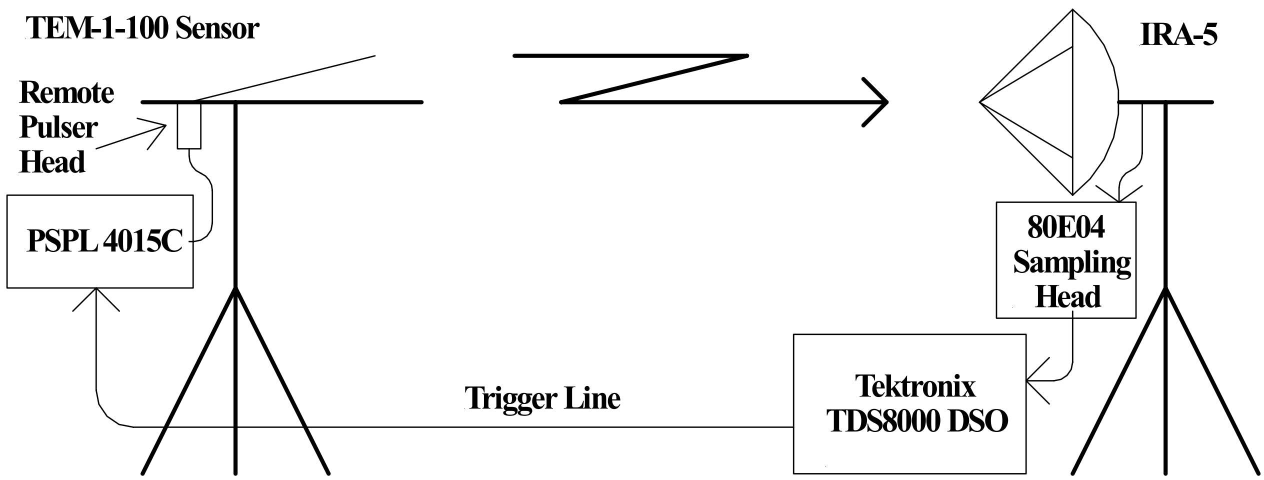

Figure 4.2. Instrumentation setup to measure the response of the IRA-5.

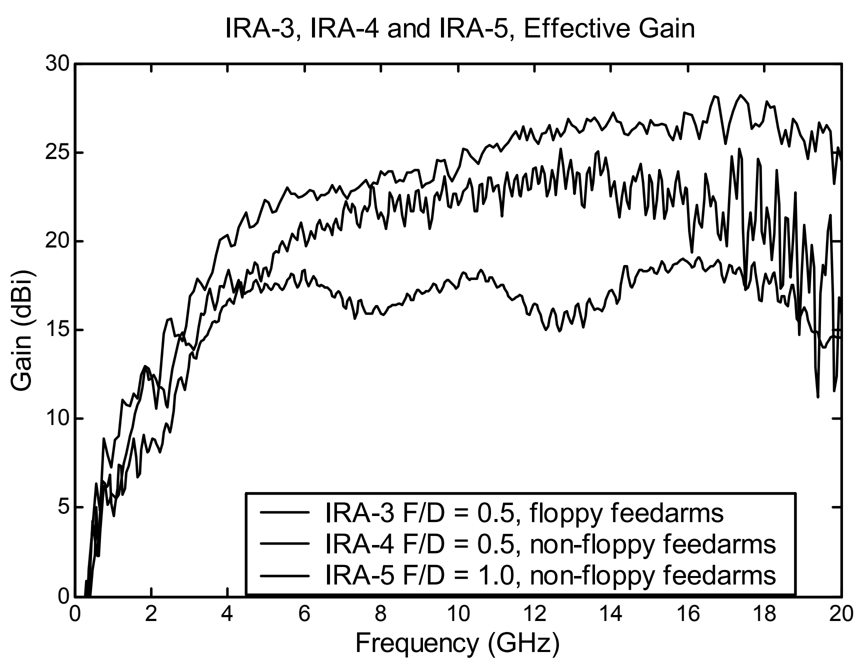

Figure 4.3. Effective gain of the IRA-3, IRA-4 and IRA-5 (top trace to bottom trace, respectively).

In Figures 4.4 through 4.6, we present comparisons between the IRA-3 impulse response and the IRA-5 impulse response in the time and frequency domains. Note that the IRA-5 has a larger pulse width than the IRA-3, 38 ps vs. 25 ps. The IRA-5 also has about half the peak magnitude.

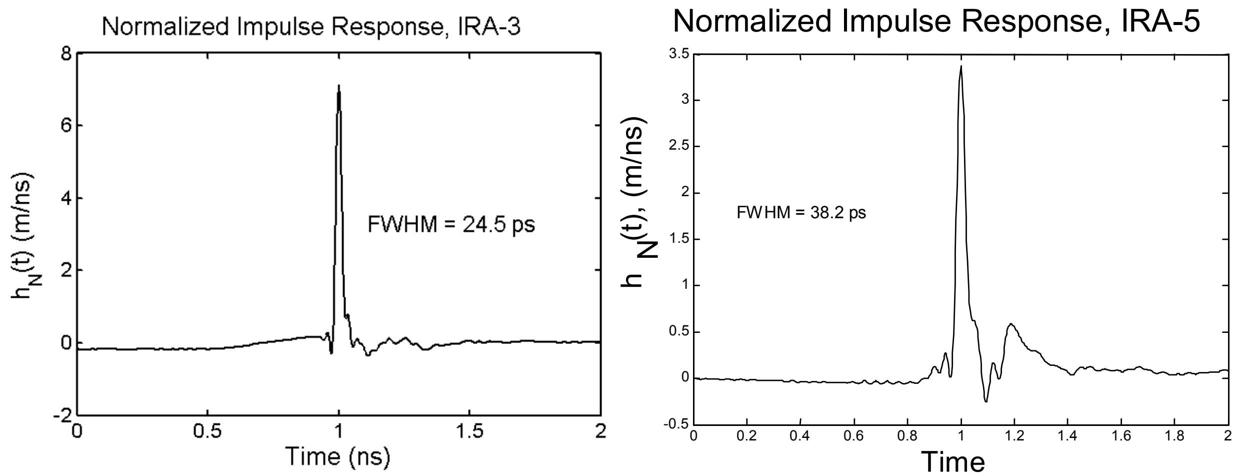

Figure 4.4. Normalized impulse responses in the time domain. (IRA-3 left, IRA-5 right)

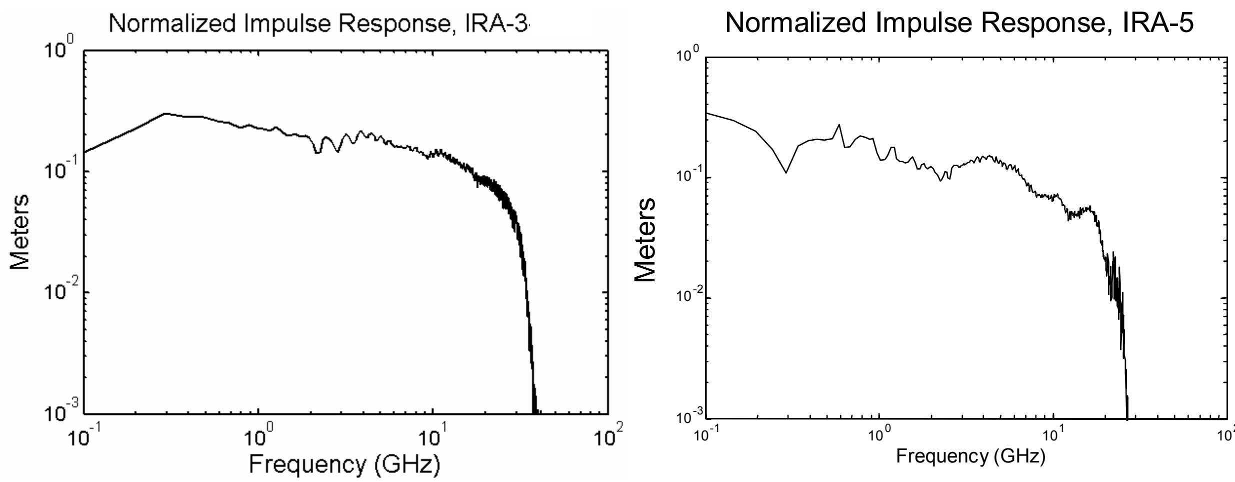

Figure 4.5. Normalized impulse responses in the frequency domain. (IRA-3 left, IRA-5 right)

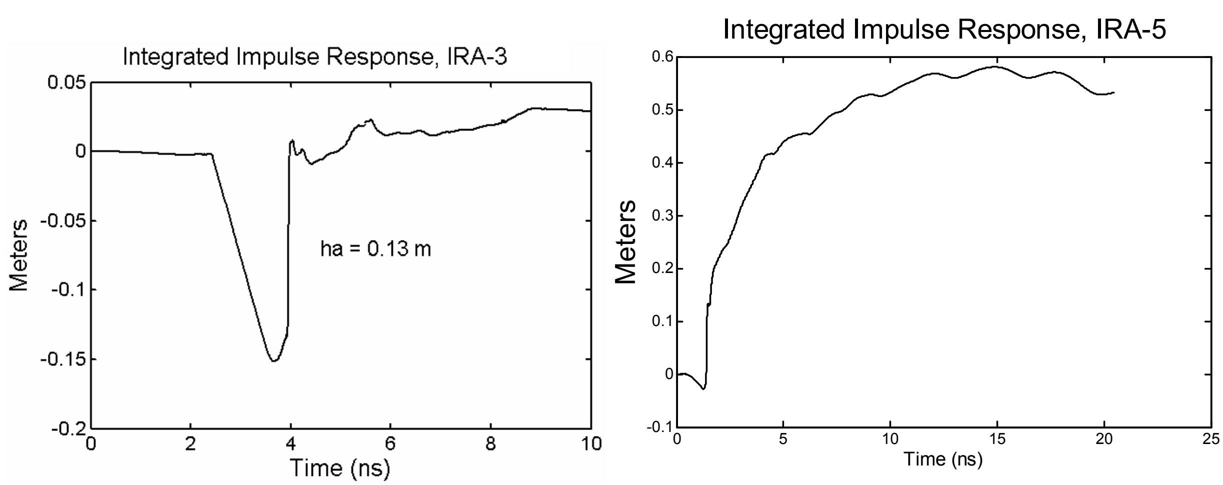

Figure 4.6. Integrated impulse responses in the time domain. (IRA-3 left, IRA-5 right)

Next, we consider the effect of varying the impedance at the end of the feed arms. Normally we terminate the feed arms in the characteristic impedance of the feed arms, 200 ohms. If we could eliminate the fabric resistors on the Para-IRA, it would simplify fabrication. To see the effect of eliminating the termination resistors, we shorted the IRA-5 termination with copper tape and measured the gain. We then removed (opened) the terminating resistors to complete the experiment. The raw received voltage for the three resistor configurations is provided in Figure 4.7, where we see that the peak voltages do not vary greatly. Shorting the termination reduces the peak output by about 10 percent.

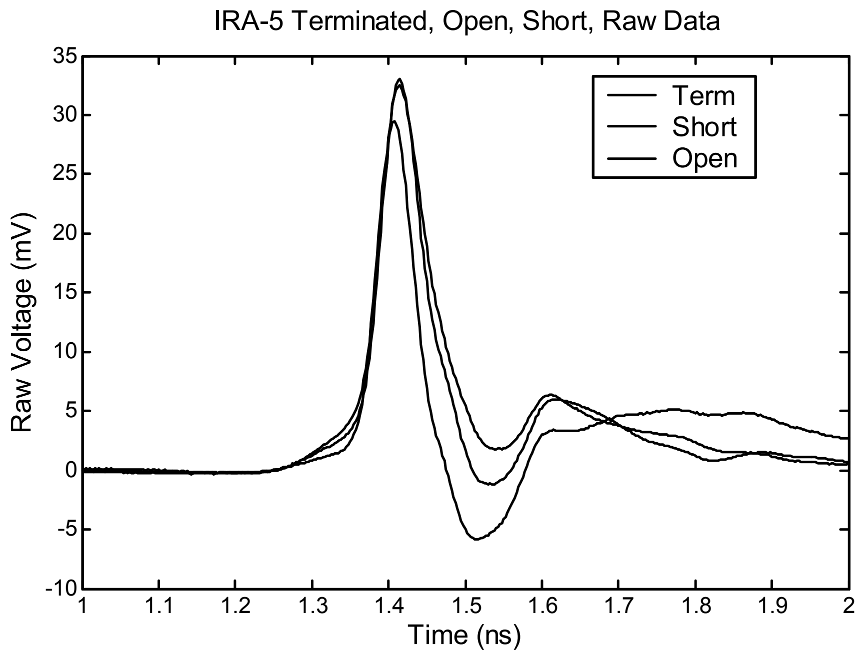

Figure 4.7. Comparison of the raw data for the three terminations.

We present the effective gain for the three terminations in Figure 4.8. Shorting the termination significantly reduces the gain below 2 GHz. Gains between 2 and 10 GHz do not vary significantly. Shorting out the terminating resistors reduced the peak raw voltage and the low-frequency gain. This may be a significant effect for the Para-IRA, because we need high gain at lower frequencies. Terminating the feed arms in an open circuit does not seem to have a major effect on the antenna, although it may have a detrimental effect on the pulser. For this reason, we recommend that the antenna feed arms be terminated in 200-ohms.

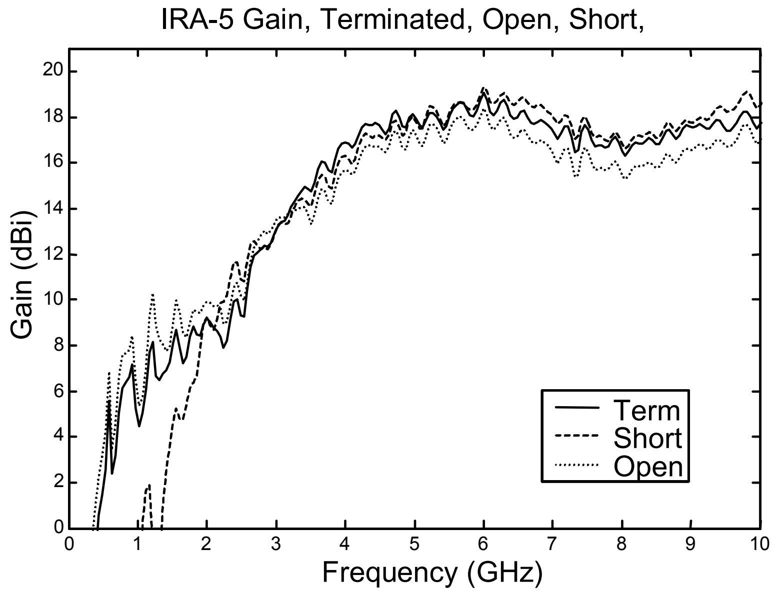

Figure 4.8. Comparison of the effective gain for the three terminations.

Next we consider the effect of aperture trimming by comparing the IRA-5b to the IRA-5. The raw data – the unprocessed voltage recorded on the oscilloscope – is shown in Figure 4.9. We see that the peak raw voltage for the IRA-5b is only slightly higher than that of the IRA-5. The effective gains for the two IRA-5's are shown in Figure 4.10. Here, we observe an advantage in trimming the aperture that ranges from 0 to 3 dB. It therefore seems useful to trim the aperture if the cost is not too great.

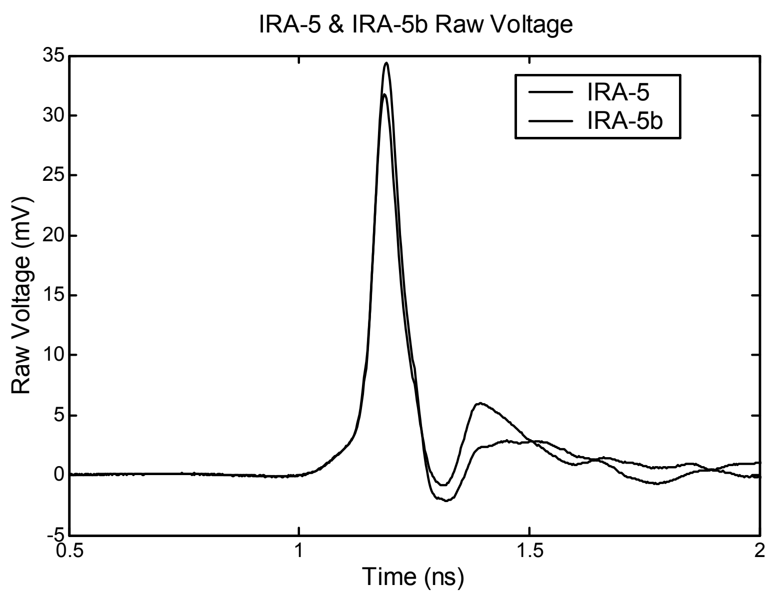

Figure 4.9. Raw voltage for the IRA-5 and IRA-5b.

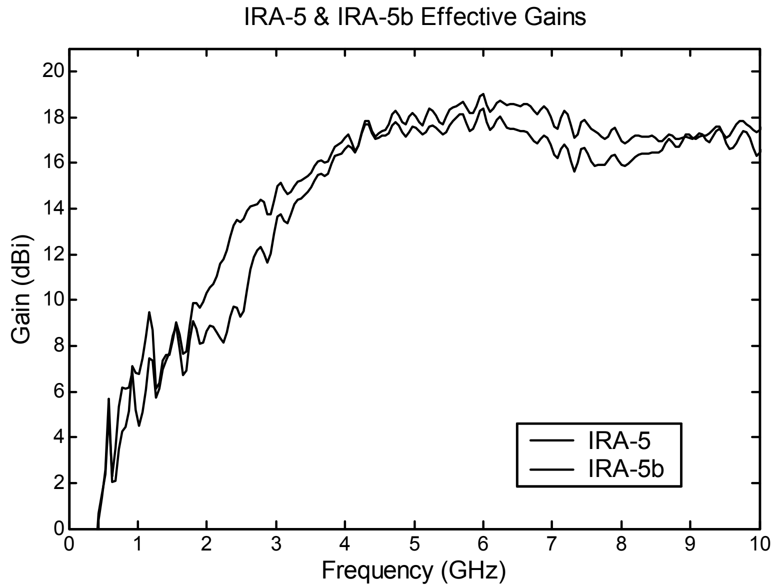

Figure 4.10. Effective gain for IRA-5 and the IRA-5b.

With the above experimental data, we can now calculate the effect of aperture trimming on the normalized aperture height, h_a/a, as defined in [2]. Recall that this quantity is an integral of the normalized impulse response, with appropriate scaling for impedance. The results are shown in Table 4.1, where we also provide the theoretical values predicted by Tyo *et al* in [2]. Theory predicts that aperture trimming leads to an increase in h_a/a of 7.5%, and we observe an increase of 10%. However, all of our experimental values are low by a factor of around 2.5, due to the large F/D ratio in the IRA-5 designs. This same reduction in performance is also observed in a significantly lower gain in Figure 4.3.

Table 1. Aperture Height and Normalized Aperture Height

Antenna	Predicted Normalized Aperture Height, h_a/a [2]	Observed Normalized Aperture Height, h_a/a
IRA-5	0.6884	0.26
IRA-5b	0.7401	0.29

The effect of aperture trimming has been studied previously, and it is useful to compare our results to earlier results. We removed a portion of the fabric in a Para-IRA model in [1], in which little effect was detected. We also masked a portion of the aperture of an IRA-4 with absorbing material in [3], and we also saw little effect. So our experiments here are the first time that we have observed the effect predicted by Tyo, probably because the geometry has been more carefully controlled.

V. Full-Scale Para-IRA Description

We also built and tested a new version of the full-size Para-IRA with fabric reflector and feed arms. This version includes a number of improvements over the original version described previously in [1]. We describe here the improvements made in the construction of the version of the Para-IRA, and we measure its antenna response. Like the previous version, this version is 1.22 meters (48 inches) in diameter with $F/D = 1$. In Figure 5.1 we show two views of the new version mounted on a wood frame for electrical testing. In Figure 5.2 we show a close-up of the feed point.

First, we consider the differences between the present version of the Para-IRA and the older version. In the present version, we used a reflector made with a fabric that is a sparse conducting mesh, Swift Textile's Leno 20 X 40, to reduce air drag. In the earlier version we simply used solid Ripstop nylon with no holes. This change increases the airflow through the reflector when the device is in flight. In doing so, air turbulence is reduced, resulting in a more stable descent and improved reflector shape. In addition, the reflector shape of the present version is more accurately controlled, because it is fabricated from twelve separate gores. Also, the present version has an improved feed point, with no material between the feed and the reflector as in the first feed point support. Finally, the present version has an open circuit at the end of the feed arms, which allows us to vary the feed arm impedance (open, short and 200 ohms) to study its effect.

In this version of the Para-IRA the conductive arms are attached to the reflector with a non-conductive fabric. This connection allows us to test various arm-to-reflector terminations, open, short and resistive, by adding conductive material or resistors.

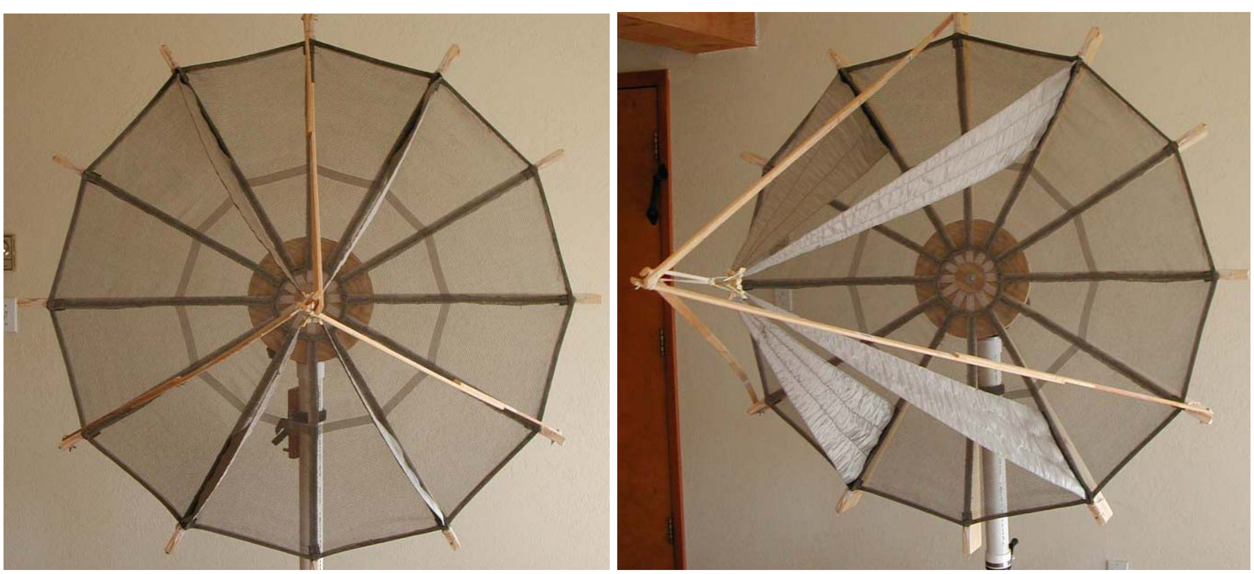

Figure 5.1. Two views of the mesh Para IRA prototype before improved feed point installation.

Figure 5.2. A close-up of the feed point of the new Para-IRA.

To connect the mesh prototype to the cable, we soldered the brass tips on the feed arms to an SMA right-angle-bend connector. We then attached to this connector a length of 0.141-inch diameter semi-rigid cable. Note that this connection leaves out the zipper balun that we expect to use in the final version. We chose to make the connection this way in order to isolate the antenna characteristic from that of the balun.

VI. Para-IRA Measurements

We begin our measurements of the Para-IRA with the TDR, as shown in Figure 6.1. Since there is no balun, the TDR starts at the 50-ohm impedance of the cable, and quickly rises to the impedance of the feed arms (~175-180 ohms). The solder connection is the discontinuity at 1 nanosecond on the graph. The feed arm impedance is seen between 1 and 9 nanoseconds at 175 – 180 ohms.

For this TDR measurement, the feed arms are open-circuited. The ends of the feed arms are sewn to a 2.5-centimeter (1-inch) wide strip of nonconductive cloth, which is sewn to the reflector. The 1-inch gap is highly capacitive and appears as a low impedance of about 100 ohms (between 9 and 10 nanoseconds) before the final termination appears. For this particular TDR, the terminating gap was unmodified, so the impedance beyond the end of the data continues to rise to an open circuit at late time.

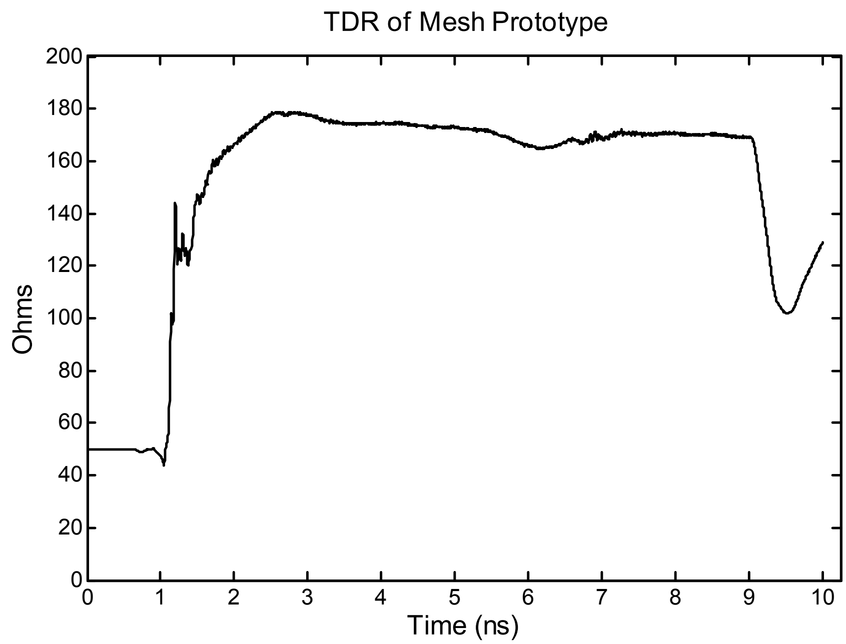

Figure 6.1. TDR of Mesh Prototype.

Next, we characterized the antenna with the instrumentation setup in shown previously in Figure 4.2. In these measurements, the antenna separation was slightly less for this test than that used in the earlier Para-IRA measurement in [1], 7 meters versus 9.5 meters. A shorter range was necessary because we performed all testing indoors due to windy conditions outdoors. The antenna height was 2 meters.

We measured the normalized impulse response with feed arms terminated in resistors, and the results are provided in Figure 6.2 in both the time and frequency domains. We also measured the gain on boresight for the three feed arm terminations: open, short and terminated. The effective gains are shown in Figures 6.3 through 6.5. These curves are somewhat lower than that observed with the original fabric Para-IRA. Also, the high-end response begins rolling off at a lower frequency, 6 GHz, than the original Para-IRA, which performed well as high as 15 GHz. This is largely inconsequential for our purposes, since the frequency range of our Marx generators is expected to be well under 5 GHz. A portion of the discrepancy can be explained by the shorter antenna range, but it seems unlikely that this explains all of it. This may also be explained in part by the use of a mesh reflector instead of a continuous ripstop nylon reflector. We also observe some unevenness in the low-frequency response, for which we can offer no explanation.

Finally, we measured the antenna pattern in the principal planes, as shown in Figures 6.6 and 6.7. We provide the pattern both in terms of raw recorded data and in terms of the normalized impulse response. Because we have plotted only the peak value, the broad pattern at low frequencies has been masked. We would expect the pattern at low frequencies to be similar to that provided in [1].

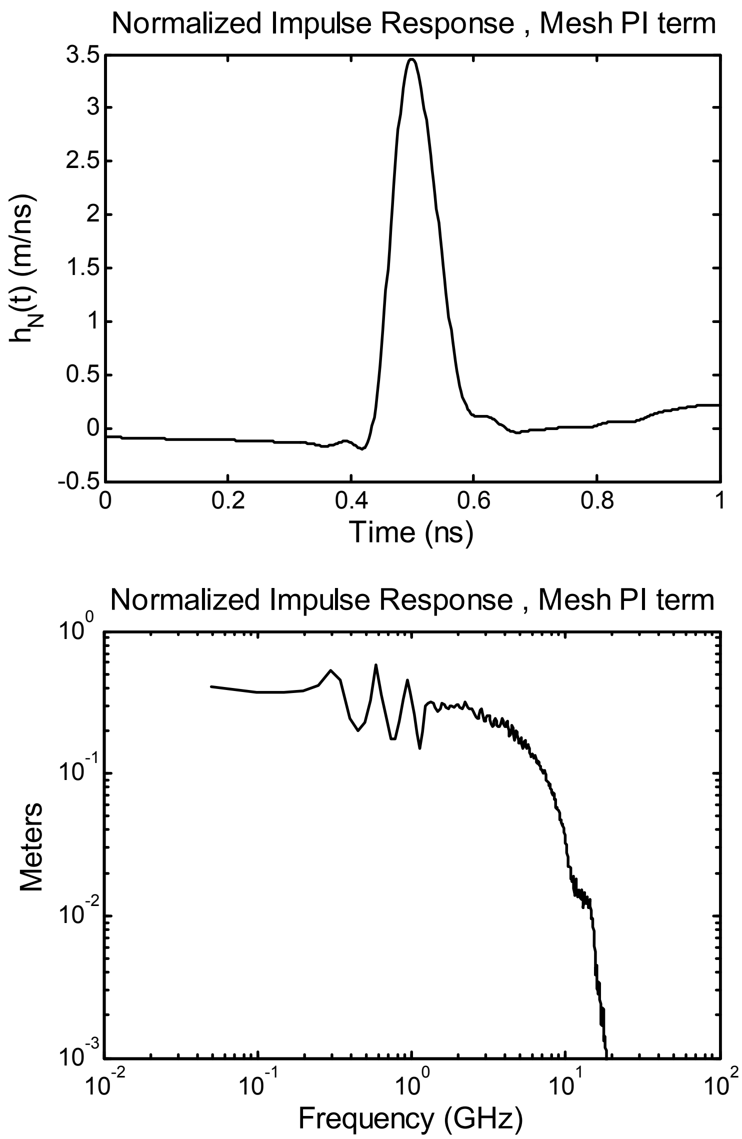

Figure 6.2. The normalized impulse response of the Para-IRA with feed arms terminated in 185 ohms, in both the time domain (top) and in the frequency domain.

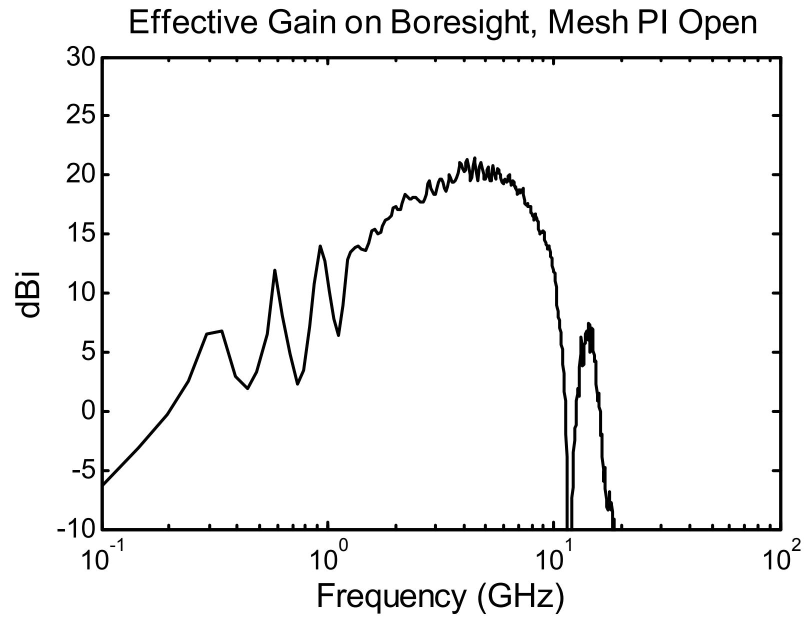

Figure 6.3. The effective gain of the mesh prototype on boresight, with feed arms left open.

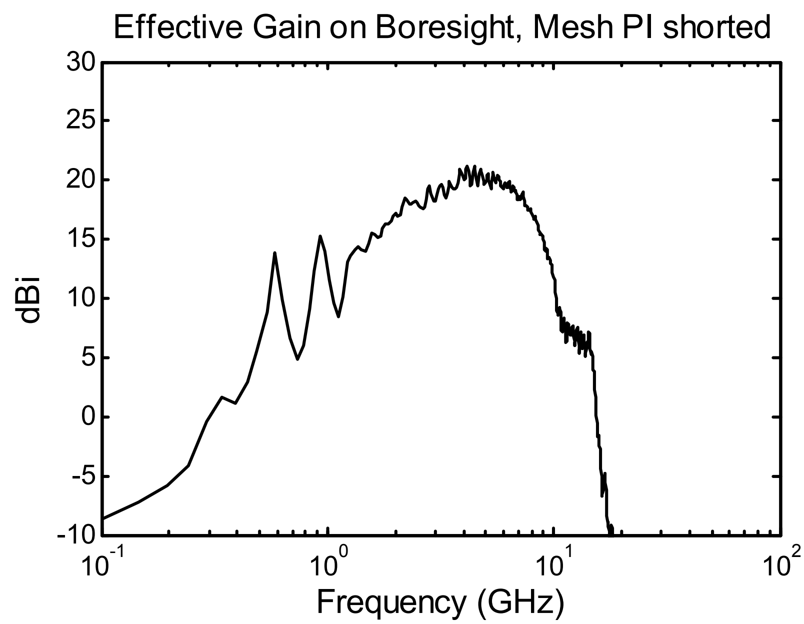

Figure 6.4 The effective gain of the mesh prototype on boresight, with feed arms shorted to the reflector.

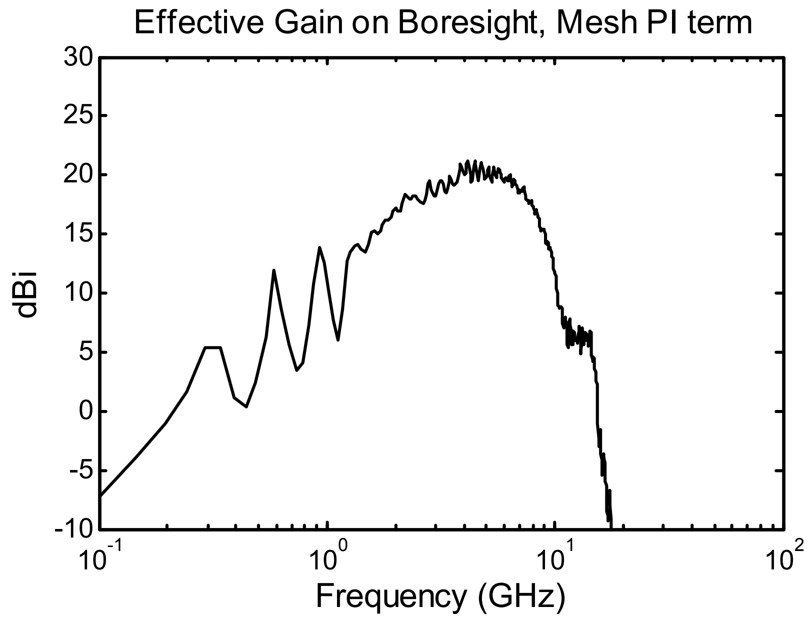

Figure 6.5. The effective gain of the mesh prototype on boresight, with feed arms terminated in 185-ohm resistors.

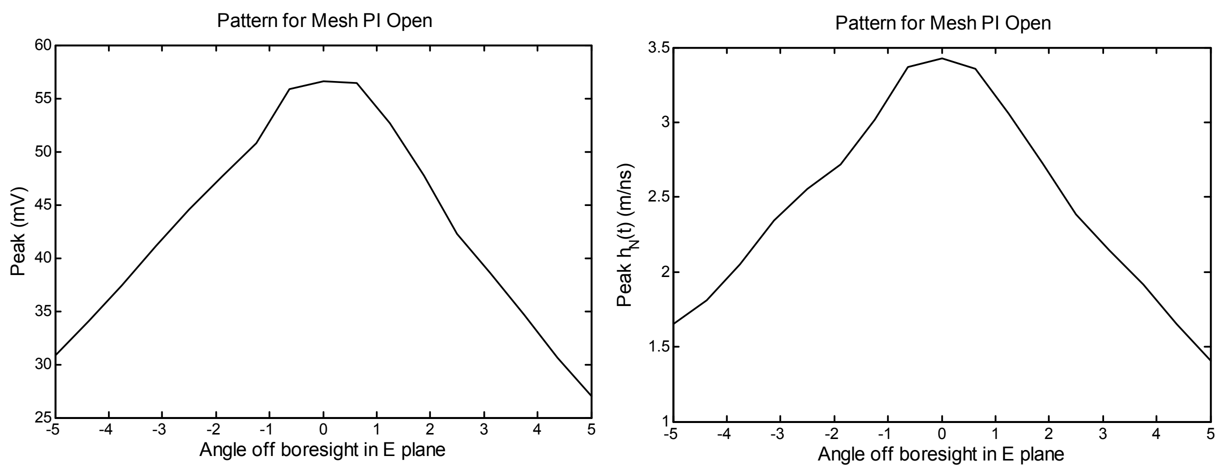

Figure 6.6. E-plane peak raw data and impulse response patterns, with feed arms open.

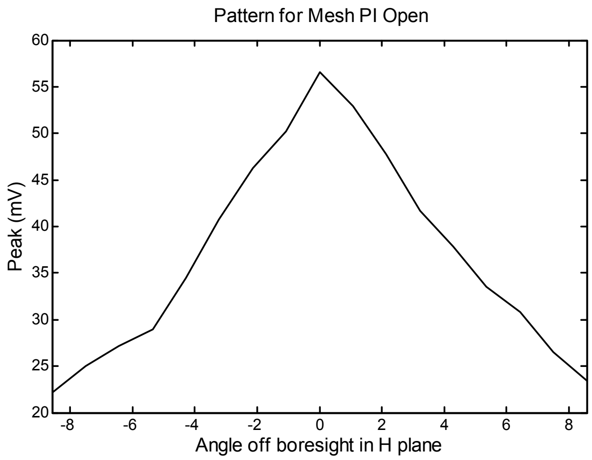

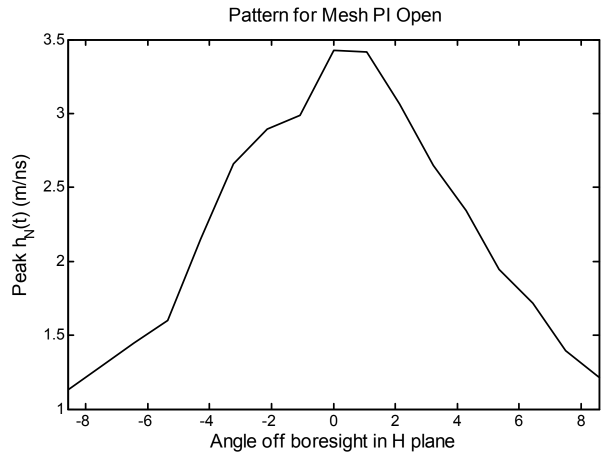

Figure 6.7. H-plane peak raw data and impulse response patterns, with feed arms open.

VII. Conclusions

As we add features to an IRA that make it more suitable for Para-IRAs, we observe a number of changes in the antenna performance parameters. We have quantified here some of these changes, so we will be better able to predict radiated fields. Using a larger *F*/*D* ratio creates more aperture blockage, thereby reducing performance. Moving the feed arms to the non-floppy position also reduces performance. Trimming the aperture increases the radiated field by 7.5 to 10 percent. Thus, it is advisable to trim the aperture in cases where the added cost is modest.

We also studied the effect of varying the impedance loading on the feed arms. In our measurements we observed little difference between open-circuited and terminated feed arms. However, short-circuited feed arms significantly reduced both the radiated peak and low-frequency response. Open-circuited feed arms have the disadvantage that they increase the voltage reflected back into the source, which may cause breakdown. So a resistive termination is the preferred configuration.

Finally, we built and tested a fabric version of the Para-IRA with a diameter of 1.22 meters (48 in.). This is an improved version of the fabric Para-IRA described in [1]. We measured the boresight gain in as a function of the impedance of the feed arms. We found the effective gain on boresight to be slightly lower than that of the earlier model. Furthermore, the high end response of this version begins to roll off at 6 GHz, as compared to 15 GHz on the earlier version. One possible explanation of this may be the use of a mesh reflector in place of the continuous fabric reflector used previously. A second possible explanation may be simply that the measurement had to be performed on a shorter antenna range than was previously used. In any case, the loss of high-end frequency response is of little consequence to the intended application, due to the limited frequency range of the intended source. We also observe some unevenness in the low-end response, which we are at a loss to explain. It is hoped that future work may resolve this question.

Acknowledgements

We wish to thank the U.S. Army Space and Missile Defense Command for funding this work.

References

1. L. M. Atchley, E. G. Farr, J. Scott Tyo, and Larry L. Altgilbers, Development and Testing of a Parachute Deployable Impulse Radiating Antenna, Sensor and Simulation Note 465, March 2002.

2. J. S. Tyo, E. G. Farr, L. H. Bowen, and L. L. Altgilbers, IRA Variations Useful for Flexible Feed Arms, Sensor and Simulation Note 472, March 2003.

3. L. H. Bowen and E. G. Farr, Results of Optimization Experiments on a Solid Reflector IRA, Sensor and Simulation Note 463, January 2002.